


ORIGINAL ARTICLE

Ultrasound evaluation of fetal bone development in the collared (*Pecari tajacu*) and white-lipped peccary (*Tayassu pecari*)

Thyago Habner de Souza Pereira¹ | Frederico Ozanan Barros Monteiro¹  |
 Gessiane Pereira da Silva¹ | Sandy Estefany Rodrigues de Matos¹ |
 Hani Rocha El Bizri^{2,3,4,5} | João Valsecchi^{2,3,4} | Richard E. Bodmer⁶ | Pedro Pérez Peña⁷ |
 Leandro Nassar Coutinho¹ | Carlos López Plana⁸ | Pedro Mayor^{1,3,6,8}

¹Federal Rural University of the Amazon (UFRA), Postgraduate Program in Animal Health and Production in Amazonia (PPGSPAA), Belém, Brazil

²Mamirauá Sustainable Development Institute (IDSM), Tefé, Brazil

³ComFauna, Comunidad de Manejo de Fauna Silvestre en la Amazonía y en Latinoamérica, Iquitos, Peru

⁴Rede de Pesquisa sobre Diversidade, Conservação e Uso da Fauna na Amazônia (REDEFAUNA), Manaus, Brazil

⁵Faculty of Humanities and Social Sciences, School of Social Sciences, Oxford Brookes University, Oxford, UK

⁶Museo de Culturas Indígenas Amazónicas, Iquitos, Peru

⁷Instituto de Investigaciones de la Amazonía Peruana (IIAP), Iquitos, Peru

⁸Facultat de Veterinària, Departament de Sanitat i d'Anatomia Animals, Universitat Autònoma de Barcelona (UAB), Barcelona, Spain

Correspondence

Frederico Ozanan Barros Monteiro,
 Avenida Presidente Tancredo Neves, N°
 2501 Bairro: Terra Firme, Cep: 66.077-830
 Cidade: Belém-Pará-Brazil.
 Email: fredericovet@hotmail.com,
frederico.monteiro@ufra.edu.br

Funding information

Conselho Nacional de Desenvolvimento Científico e Tecnológico, Grant/Award Number: 201475/2017-0, 441435/2007-3 and 452908/2016-7; Coordenação de Aperfeiçoamento de Pessoal de Nível Superior, Grant/Award Number: 021/2018 Procad Amazônia; Fundação Amazônia

Abstract

The study of fetal development allows for evaluating the different strategies adopted by mammal species to maximize neonatal survival. Autonomous locomotion is fundamental for newborns to perform foraging activities and increases newborn survival from predation. In this study, we assess the gestational bone development of 53 collared (CP, *Pecari tajacu*) and 61 white-lipped (WLP, *Tayassu pecari*) peccaries, collected through the collaboration of subsistence hunters in the Amazon. The bone mineralization and biometry of the axial and appendicular skeleton were assessed by ultrasound examinations, and the timing of the main bone developmental events was calculated in relation to the total dorsal length (TDL) and the percentage of the total gestational period (GP). The first US signs of mineralization of the axial skeleton in CP and WLP were observed in fetuses with 3.4 cm (42 gestation days, 30% GP_{CP}) and 5.1 cm (51 gestation days, 32% GP_{WLP}). The early development of the appendicular skeleton was observed by the synchronic appearance of the mineralized scapula, humerus, radius, ulna, ilium, ischium, femur, tibia, and fibula at 36% GP_{CP} (50 gestation days), and 35% GP_{WLP} (56 gestation days). The pubis was mineralized in fetuses at 55% GP_{CP} (75 gestation days) and 59% GP_{WLP} (94 gestation days). The mineralization was observed in all autopod bones at 79% GP_{CP} (109 gestation days) and 67% GP_{WLP} (106 gestation days). All primary ossification centers in long bones of thoracic and pelvic limbs were mineralized in advanced fetuses (GP_{CP and WLP} ≥75%). The mineralized patella was not observed in advanced fetuses in either species. Secondary ossification centers first appeared at the distal epiphysis of the femur in the CP (99 gestation days, 72% GP_{CP}) and the distal epiphysis of the radius, femur, and tibia in the WLP (106 gestation days, 67% GP_{WLP}). Advanced fetuses of CP and WLP presented 60% (15/25) and 68% (17/25) of the total secondary ossification centers observed present in the adult domestic pig, while newborns from the domestic pig presented 52% (13/25). The early intrauterine development of the skeletal system in both peccary species suggests a

Paraense de Amparo à Pesquisa, Grant/Award Number: 06/2015; Fundação de Amparo à Pesquisa do Estado do Amazonas, Grant/Award Number: 016/2014

precocial development strategy, which likely correlates with neonatal ability to escape predators and reduces the dependence on parental care.

KEYWORDS

bone, fetal development, precocity, skeletal system, Tayassuidae

1 | INTRODUCTION

Peccaries are even-toed ungulates belonging to the order Artiodactyla, family Tayassuidae, which includes the collared peccary (CP, *Pecari tajacu*), the white-lipped peccary (WLP, *Tayassu pecari*), and the Chacoan peccary (*Catagonus wagneri*). They occur in the southern United States, Central America, and most South American countries (Sowls, 1997; Tiepolo & Tomas, 2006). According to the IUCN, CP is classified as a Least Concern species, while the WLP is Vulnerable to extinction (Gongora et al., 2011; Keuroghlian et al., 2013). Despite the extensive distribution of these two species, high hunting pressure and habitat fragmentation can promote substantial population reductions (Fang et al., 2008).

Peccary females are polyoestrous (Gottdenker & Bodmer, 1998; Mayor, Fenech, et al., 2006; Mayor, Lopez-Gatius, et al., 2006), with a mean gestation length of 138 days in the CP (Mayor et al., 2005) and 156–162 days in the WLP (Roots, 1966). The reproductive output in the wild is 1.7–1.9 and 1.6–1.7 neonates per gestation in the CP and WLP, respectively (Gottdenker & Bodmer, 1998; Mayor et al., 2009). Recent studies have demonstrated a high precociality in the CP (Mayor et al., 2019) and the WLP (Andrade, Monteiro, El Bizri, et al., 2018), with well-developed external and internal characteristics in newborns. However, there is still a great lack of knowledge on fetal bone development and the role of the musculoskeletal system in the early life history of these species.

Skeletal bones support the body and are considered the passive organs of movement, allowing specimens to move in combination with muscles (Dyce et al., 2010). Studying the skeletal system development during the uterine period allows comparing the level of neonatal independence among species, and understanding strategies adopted by different species to optimize neonatal survival (Clancy et al., 2001; Derrickson, 1992; Francioli et al., 2011). This study assesses the gestational development of the axial and appendicular skeleton of the CP and WLP, including the first US signs of mineralization of the primary and secondary ossification centers and subsequent bone growth. The results of this study are useful to standardize parameters for the monitoring of fetal development and improve the understanding of life history strategies of precocial mammals.

2 | MATERIALS AND METHODS

2.1 | Study sites

This study was conducted in three locations in the Amazon Forest. Two sites were located in the northeastern Peruvian Amazon: the Yavarí-Mirín River (S 04°19.53; W 71°57.33) and the Pucacuro

National Reserve (S 02°23.45; W 75°14.16), and one site, the Amaná Sustainable Development Reserve (S 01°54.00; W 64°22.00), was located in the central Brazilian Amazon, between the Negro and Japurá rivers.

2.2 | Biological sample collection and processing

From 2000 to 2015, local hunters collected and voluntarily donated the reproductive tracts of CP and WLP females. Hunters were trained to remove all abdominal and pelvic organs with the perineal region from hunted specimens and to store these in buffered 4% formaldehyde solution (v/v) (Mayor et al., 2017). All reproductive tracts were obtained through usual activities of subsistence hunting, and no animal was captured solely for the purpose of this study.

Reproductive tracts of pregnant females were dissected to remove all conceptuses. In this study we included all fetuses from single pregnancies, and, in the case of twins, we randomly selected only one conceptus. A total of 53 conceptuses (7 embryos and 46 fetuses) of CP and 61 conceptuses (2 embryos and 59 fetuses) of WLP were analyzed. The embryonic and fetal phases were determined according to the International Committee on Veterinary Embryological Nomenclature (2017). The embryos were identified by the absence of eyelids and identification of genital tubercle, interdigital webbing, and limb buds, while the fetuses were characterized based on the differentiation of external genitalia and the presence of eyelids and limbs. The total dorsal length (TDL), crown-rump length (CRL), and body mass were measured in all conceptuses (Table S1). The TDL was obtained using a tape measure (0.1 mm accuracy) and the CRL was measured with a metal caliper (full measurement capacity 300 mm), while the body mass was quantified using a digital scale (0.1 g accuracy) (Table 1). All measurements were performed in triplicate by the same researcher and the mean values were calculated.

The research protocol was approved by the Research Ethics Committee for Experimentation in Wildlife at the Dirección General de Flora y Fauna Silvestre from Peru (License 0229-2011-DGFFS-DGEFFS), by the Head of the National Reserve of Pucacuro (03-2012-SERNANPRN Pucacuro), by the Chico Mendes Institute for Biodiversity Conservation from Brazil (License SISBIO N° 29,092-1), and by the Committee on Ethics in Research with Animals of the Federal Rural University of the Amazon (CEUA/UFRA protocol 008/2016). Samples were sent to UFRA, Belém, Pará, Brazil using the export license CITES / IBAMA (No. 14BR015991/DF).

2.3 | Ultrasound examination

B-mode ultrasound evaluations were performed with Esaote® ultrasound equipment, model MyLab™ 30 Vetgold equipped with a linear and multifrequency transducer (10–18 MHz). The embryos/fetuses were immersed in water and the transducer was maintained in direct contact (underwater) with the evaluated fetal surface. A video portraying the method of the ultrasound examination is presented as Supplementary Material.

Although we did not establish the relationship between echogenicity and mineralization, ultrasonography is a well-validated technique and largely used for detecting mineralization and measuring fetal bones and ossification centers (Donne et al., 2005; Mahoney et al., 1985; Moradi et al., 2019). In ultrasound, the cartilage is observed as a homogenous anechoic region and is characterized by the absence of mineralization. The development of diaphysis is characterized by delimited hyperechoic structures and the ossification centers are detected as light grey spots within the cartilages (Karami et al., 2016).

The ultrasonography evaluation was based on the methodology proposed by Silva et al. (2020). The skull was evaluated at the sagittal section of the interthalamic level to obtain the biparietal diameter (BPD), occipitofrontal diameter (OFD), and head circumference (HC). The BPD was measured in the largest transversal diameter of the parietal bones and the OFD was obtained as the perpendicular distance from the BPD, respecting the limits of the frontal and occipital bones. The HC was measured by a contour around the hyper-echogenic border of the skull (Figure 1). The vertebral column was divided into five portions for evaluation (cervical, thoracic, lumbar, sacral, and caudal) and these were examined by the presence of the mineralized vertebral body in longitudinal sections. The ribs were identified by the transducer positioned in the longitudinal and transverse planes.

Examination of the thoracic limb was performed starting from the scapula in the proximal region of the limb, with the transducer on the scapular spine in the longitudinal section. The length of the mineralized part, total length (including mineralized and non-mineralized parts), and the width (lateromedial diameter) were evaluated at the distal portion of the bone in contact with the scapulohumeral joint. Afterward, the humerus, radius, and ulna were successively evaluated, keeping the transducer axis as close as possible to a right angle with the bone structure, and observing the cartilaginous epiphyses. The mineralized diaphysis (hyperechoic part), the proximal and distal extremities (epiphysis, hypoechoic part), width (lateromedial diameter), total length (diaphysis and epiphyses), and secondary ossification center were measured. The carpal bones were quantified and the length and width of the mineralized part in the metacarpi and phalanges (proximal, middle, and distal) were measured (Figure 2).

The evaluation of the pelvic limb was conducted similarly to that performed on the thoracic limb, assessing the total length (mineralized and non-mineralized parts), the length of the mineralized parts, and width (near to acetabulum) of the ilium and ischium. In the pubis,

the length and width of the mineralized parts were evaluated (Silva et al., 2020). The examination of the femur, tibia, and fibula was similar to the humerus (Figure 3). Besides, the mineralization of the tarsal bones was evaluated, measuring the length and width of the calcaneus and talus. Regarding the metatarsi and phalanges, the length and width of the mineralized parts were obtained.

In the secondary ossification centers, we measured the largest and smallest perpendicular diameters in the sagittal plane. All measurements were performed in triplicate and the mean values were calculated.

2.4 | Data analysis

The gestational age (GA) of the CP was estimated using the formula $^3\sqrt{W} = 0.079 (t-27.6)$ proposed by Mayor et al. (2019), while for the WLP we used the formula $^3\sqrt{W} = 0.084 (t-31.8)$ presented by Andrade, Monteiro, El Bizri, et al. (2018), where W is the fetal weight and t the fetal age in days. The relationship of GA with TDL, CRL, and body mass in all conceptuses was established through linear regressions. The timing of the main events of the bone development was expressed in terms of GA (days) and percentage of the total gestational period (GP).

Comparative evaluations concerning the percentage of secondary ossification centers were conducted based on the total number of secondary ossification centers observed in the adult domestic pig, which has a total of 25 secondary ossification centers (Barone, 2010; Dyce et al., 2010).

Logistic regressions were used to estimate the probability of mineralization in primary and secondary ossification centers with TDL using the software Statistica 8.0 (StatSoft Inc.). Multiple linear and non-linear regressions modeling relationships between TDL and biometric measures were applied using the CurveExpert Professional 2.8 software (© Copyright 2017, Daniel G. Hyams), which defined the best functions for the plots, considering zero the day 0 of the gestational period. In addition, allometric relationships between the length and width of long bones (humerus, radius, femur, and tibia) were evaluated in comparison to TDL. The value of $p < 0.05$ was considered significant.

3 | RESULTS

The mean TDL_{CP} for all conceptuses was 14.9 ± 8.9 cm (range 1.5–32.8 cm), the mean CRL_{CP} was 10.8 ± 6.3 cm (range 1.5–24.1 cm), and the mean body mass was 174 ± 200 g (range 0.6–745 g) (Table S1). The GA of CP conceptuses showed a high positive linear relationship with TDL ($r^2 = 0.95$, $p < 0.01$), CRL ($r^2 = 0.97$, $p < 0.01$) and body mass ($r^2 = 0.91$, $p < 0.01$; Figure 4a,c,e).

The mean TDL_{WLP} was 20 ± 10.3 cm (range 2.0–38.6 cm), the mean CRL_{WLP} was 14.6 ± 7.7 cm (range 1.3–28.7 cm), and the body mass was 360.1 ± 396.9 g (range 0.2–1288 g). The GA of WLP conceptuses presented a high positive linear relationship with TDL

TABLE 1 Logistic equations [$y = \exp(\text{intercept} + \text{estimate} \times x) / (1 + \exp(\text{intercept} + \text{estimate} \times x))$] for the axial and appendicular bone parameters in 53 collared (*Pecari tajacu*; left column) and 61 white-lipped peccary (*Tayassu pecari*; right column) embryos/fetuses

Bones	Collared peccary (N = 53)				White-lipped peccary (N = 61)			
	Intercept	Estimate	Chi-square (df)	p value	Intercept	Estimate	Chi-square (df)	p value
Axial bones (skull; spine; ribs)								
Skull	-5.106	1.320	33.3333 (1)	<0.001	-4.423	1.0798	14.9662 (1)	<0.001
Cervical	-6.919	1.345	41.0513 (1)	<0.001	-6.141	1.1437	24.1472 (1)	<0.001
Thoracic	-6.919	1.345	41.0513 (1)	<0.001	-6.141	1.1437	24.1472 (1)	<0.001
Lumbar	-6.919	1.345	41.0513 (1)	<0.001	-6.141	1.1437	24.1472 (1)	<0.001
Sacral	-6.919	1.345	41.0513 (1)	<0.001	-6.141	1.1437	24.1472 (1)	<0.001
Caudal	-8.864	1.405	47.5521 (1)	<0.001	-7.813	1.1655	36.8700 (1)	<0.001
Ribs	-6.919	1.345	41.0513 (1)	<0.001	-6.141	1.1437	24.1472 (1)	<0.001
Appendicular bones (forelimb)								
Scapula	-6.859	1.333	41.0196 (1)	<0.001	-6.733	1.1539	27.9985 (1)	<0.001
Humerus	-6.859	1.333	41.0196 (1)	<0.001	-6.733	1.1539	27.9985 (1)	<0.001
Radius	-7.797	1.356	43.6749 (1)	<0.001	-7.483	1.1810	32.1003 (1)	<0.001
Ulna	-7.797	1.356	43.6749 (1)	<0.001	-7.483	1.1810	32.1003 (1)	<0.001
Proximal carpus	-83.945	3.707	55.1148 (1)	<0.001	-24.371	1.6203	74.3580 (1)	<0.001
Distal carpus	-83.945	3.707	55.1148 (1)	<0.001	-24.371	1.6203	74.3580 (1)	<0.001
Metacarp	-15.286	1.588	61.9896 (1)	<0.001	-12.052	1.2812	56.1976 (1)	<0.001
Proximal phalanx	-21.859	1.798	69.6213 (1)	<0.001	-15.772	1.3730	64.8034 (1)	<0.001
Middle phalanx	-21.859	1.798	69.6213 (1)	<0.001	-17.946	1.4550	66.8930 (1)	<0.001
Distal phalanx	-21.859	1.798	69.6213 (1)	<0.001	-17.946	1.4550	66.8930 (1)	<0.001
Appendicular bones (hind limb)								
Ilium	-7.797	1.356	43.6749 (1)	<0.001	-7.270	1.1467	32.3788 (1)	<0.001
Ischium	-7.797	1.356	43.6749 (1)	<0.001	-7.270	1.1467	32.3788 (1)	<0.001
Pubis	-19.255	1.723	57.1387 (1)	<0.001	-33.723	1.8842	66.0157 (1)	<0.001
Femur	-6.859	1.333	41.0196 (1)	<0.001	-7.270	1.1467	32.3788 (1)	<0.001
Tibia	-7.797	1.356	43.6749 (1)	<0.001	-7.270	1.1467	32.3788 (1)	<0.001
Fibula	-7.797	1.356	43.6749 (1)	<0.001	-7.270	1.1467	32.3788 (1)	<0.001
Calcaneus	-24.175	1.883	67.6478 (1)	<0.001	-19.689	1.4731	64.2953 (1)	<0.001
Talus	-43.267	2.454	63.7375 (1)	<0.001	-39.822	2.0073	70.5232 (1)	<0.001
Tarsus	-83.945	3.707	55.1148 (1)	<0.001	-46.519	2.2390	75.7515 (1)	<0.001
Metatars	-15.286	1.588	61.9897 (1)	<0.001	-8.712	1.1992	40.7693 (1)	<0.001
Proximal phalanx	-21.859	1.798	69.6214 (1)	<0.001	-13.416	1.1644	56.0695 (1)	<0.001
Middle phalanx	-21.859	1.798	69.6214 (1)	<0.001	-13.416	1.1644	56.0695 (1)	<0.001
Distal phalanx	-21.859	1.7977	69.6214 (1)	<0.001	-11.286	0.929	54.3895 (1)	<0.001

($r^2 = 0.96$, $p < 0.01$), CRL ($r^2 = 0.96$, $p < 0.01$) and body mass ($r^2 = 0.93$, $p < 0.01$; Figure 4b,d,f).

3.1 | Axial skeleton

The probability curves and equations of mineralization of the axial skeleton in both species were similar (Figure 5a,b, Table 1). No embryo presented bone mineralization in the axial skeleton. First signs

of mineralized skull (occipital, frontal, and parietal bones) were observed in fetuses with $TDL_{CP} = 3.4$ cm (42 gestation days, 30% GP_{CP}), and $TDL_{WLP} = 5.1$ cm (51 gestation days, 32% GP_{WLP}). The mineralization of cervical, thoracic, lumbar, and sacral vertebral bodies and ribs were first observed in fetuses with $TDL_{CP} = 5.7$ cm (50 gestation days, 36% GP_{CP}) and $TDL_{WLP} = 5.8$ cm (54 gestation days, 34% GP_{WLP}). The caudal vertebral bodies initiated the mineralization in fetuses with $TDL_{CP} = 7.1$ cm (55 gestation days, 40% GP_{CP}) and $TDL_{WLP} = 7.1$ cm (58 gestation days, 36% GP_{WLP}).

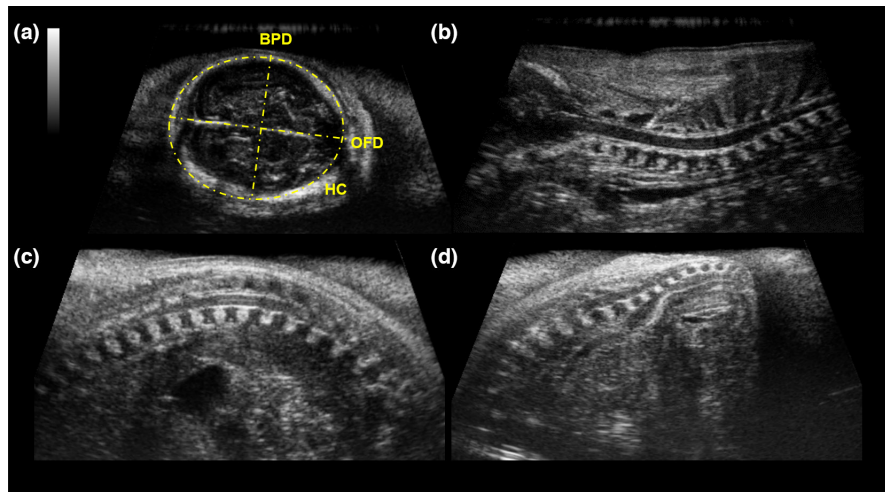


FIGURE 1 Ultrasonographic planes used for the examination of the axial skeleton of collared peccary (*Pecari tajacu*) and white-lipped peccary (*Tayassu pecari*) fetuses: (a) biparietal diameter (BPD), occipitofrontal diameter (OFD), and head circumference (HC) measurements; (b–d) sagittal fetal spine sections, (b) cervical, (c) thoracic and lumbar, (d) and sacral.

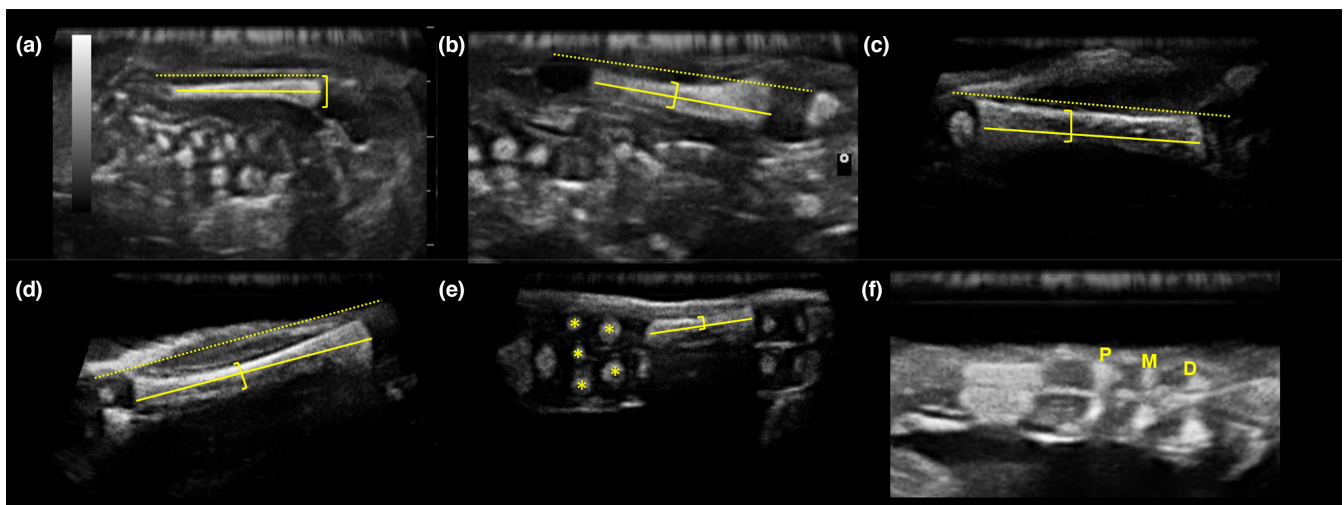


FIGURE 2 Ultrasonographic planes used for the examination and measurement of the thoracic limb of collared peccary (*Pecari tajacu*) and white-lipped peccary (*Tayassu pecari*) fetuses: (a) scapula, (b) humerus, (c) radius, (d) ulna, (e) carpal (*) and metacarpal bones, (f) proximal (P), middle (M) and distal (D) phalanges. Ossified portion/diaphysis (solid line), total length (dotted line), width (I).

The 100% probability of the first US signs of mineralization process in the skull was observed in fetuses with $TDL_{CP} \geq 7.9$ cm (58 gestation days, 42% GP_{CP}) and $TDL_{WLP} \geq 9.1$ cm (65 gestation days, 41% GP_{WLP}). The cervical, thoracic, lumbar, sacral vertebral bodies, and ribs had a 100% probability of presenting signs of mineralization in fetuses with $TDL_{CP} \geq 9.1$ cm (62 gestation days, 45% GP_{CP}), and $TDL_{WLP} \geq 10.1$ cm (68 gestation days, 43% GP_{WLP}); and caudal vertebral bodies were mineralized in all fetuses with $TDL_{CP} \geq 10.1$ cm (65 gestation days, 47% GP_{CP}) and $TDL_{WLP} \geq 11.3$ cm (72 gestation days, 45% GP_{WLP}).

3.2 | Appendicular skeleton

First signs of mineralization in bones in the thoracic and pelvic limbs were observed in fetuses with $TDL_{CP} = 5.7$ cm (50 days of gestation,

36% GP_{CP}) and $TDL_{WLP} = 6.3$ cm (55 gestation days, 35% GP_{WLP}). The signs of mineralization were first observed in the scapula, humerus, radius, ulna (thoracic limb), ilium, ischium, femur, tibia, and fibula (pelvic limb) (Figures 5c–f). Mineralization in the pubis was observed in fetuses with $TDL_{CP} \geq 13.1$ cm (75 gestation days, 55% GP_{CP}) and $TDL_{WLP} \geq 17.8$ cm (94 gestation days, 59% GP_{WLP}).

In the CP, first signs of mineralization in metacarpi and metatarsi were observed simultaneously in fetuses with $TDL_{CP} \geq 9.7$ cm (64 gestation days, 46% GP_{CP}); in the WLP, mineralization of the metatarsi was first observed in fetuses with $TDL_{WLP} \geq 7.2$ cm (58 gestation days, 37% GP_{WLP}), while metacarpi mineralization was observed in fetuses with $TDL_{WLP} \geq 9.4$ cm (66 gestation days, 41% GP_{WLP}).

In the forepaw and the hind paw of the CP, first signs of mineralization of the proximal, middle, and distal phalanges were simultaneously observed in fetuses with $TDL_{CP} \geq 13.0$ cm (75 gestation

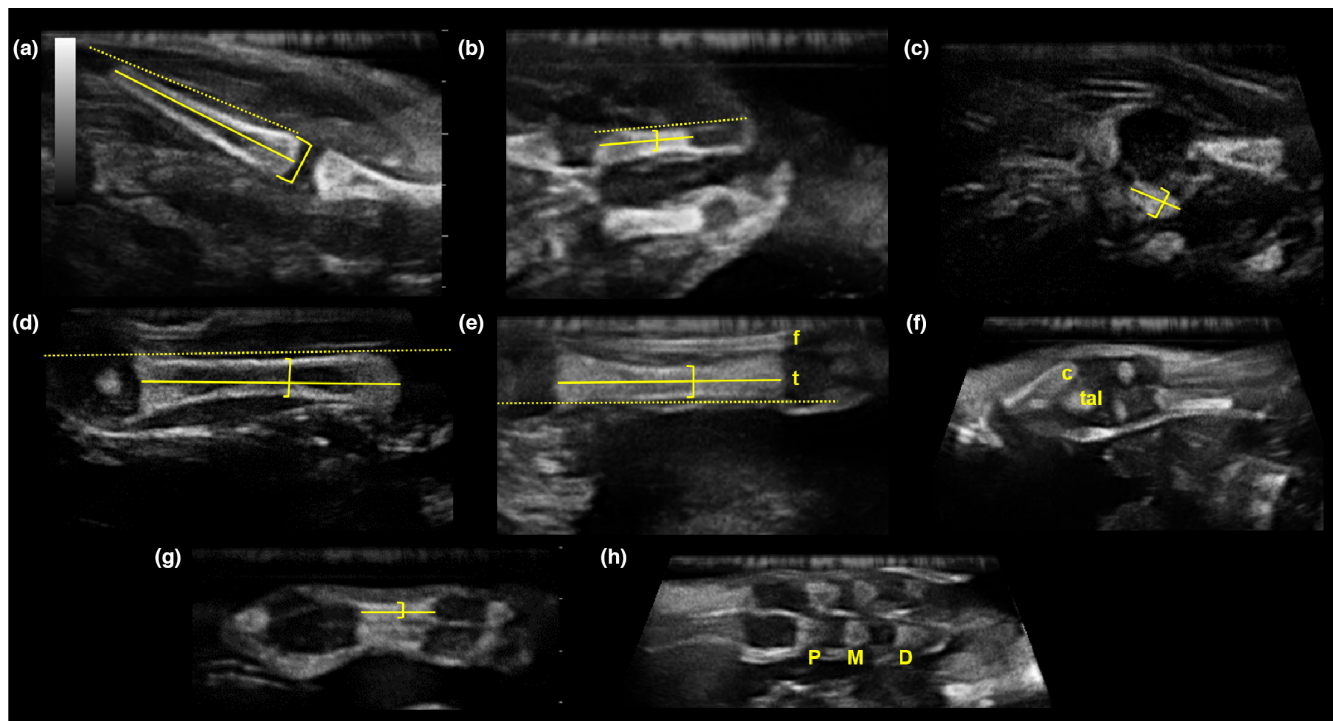


FIGURE 3 Ultrasonographic planes used for the examination and measurement of the pelvic limb of collared peccary (*Pecari tajacu*) and white-lipped peccary (*Tayassu pecari*) fetuses: (a) ilium, (b) ischium, (c) pubis, (d) femur, (e) tibia (t) and fibula (f), (f) calcaneus (c) and talus (tal), (g) metatarsal bones, (h) proximal (P), middle (M) and distal (D) phalanges. Ossified portion/diaphysis (solid line), total length (dotted line), width (J).

days, 54% GP_{CP}). In the WLP, proximal, middle, and distal phalanges of the hind paw showed first signs of mineralization in fetuses with TDL_{WLP} ≥ 11.6 cm (73 gestation days, 46% GP_{WLP}). In the forepaw, the proximal phalange was first observed mineralized in fetuses with TDL_{WLP} = 12.0 cm (75 gestation days, 47% GP), while the middle and the distal phalange showed a slight delay (TDL_{WLP} = 13.2 cm, 79 gestation days, 49% GP_{WLP}).

In CP, the mineralization in the carpal or tarsal bones was first observed in the calcaneus (TDL_{CP} ≥ 13.1 cm, 75 gestation days, 55% GP_{CP}), followed by the talus (TDL_{CP} = 17.8 cm, 92 gestation days, 66% GP_{CP}), the proximal portion of the carpal bones and the distal portion of the carpal (TDL_{CP} = 22.8 cm, 109 gestation days, 79% GP_{CP}), and, finally, the distal portion of the tarsus (TDL_{CP} = 22.8 cm, 109 gestation days, 79% GP_{CP}) (Figure 5c,e). In WLP, the mineralization in the carpal or tarsal bones also was first observed in the calcaneus (TDL_{WLP} ≥ 13.8 cm, 81 gestation days, 51% GP_{WLP}), but it was followed by the proximal portion of the carpal bones and the distal portion of the carpal (TDL_{WLP} ≥ 15.0 cm, 85 gestation days, 53% GP_{WLP}), talus (TDL_{WLP} ≥ 19.6 cm, 100 gestation days, 63% GP_{WLP}), and, finally, the distal portion of the tarsus (TDL_{WLP} ≥ 21.2 cm, 106 gestation days, 67% GP_{WLP}) (Figure 5d,f). In advanced fetuses of CP (TDL_{CP} ≥ 22.4 cm, 108 gestation days, GP_{CP} ≥ 78%) there was observed three proximal and three distal carpal bones mineralized, while in WLP (TDL_{WLP} ≥ 25.6 cm, 121 gestation days, GP_{WLP} ≥ 76%) there was observed three proximal and four distal carpal bones. Regarding the distal portion of the tarsus, CP and WLP showed two and three bones, respectively.

Mineralization in all long bones started in the middle part of the diaphysis. Fetuses with TDL_{CP} ≥ 9.7 cm (64 gestation days, 46% GP_{CP}) and TDL_{WLP} ≥ 11.0 cm (71 gestation days, 45% GP_{WLP}) had a 100% probability of mineralization in long bones of thoracic (scapula, humerus, radius, and ulna) and pelvic limbs (femur, tibia, and fibula). Mineralization in the patella was not observed in advanced fetuses of either CP or WLP (TDL ≥ 22.4 and 25.6 cm, respectively).

3.3 | Epiphyseal ossification centers

In the CP, the first US signs of mineralization in epiphyseal centers were observed in fetuses with TDL_{CP} ≥ 20.0 cm (99 gestation days, 72% GP_{CP}) (Figure 6a,c, Table 2). The early occurrence of mineralization of secondary centers was progressively observed in the distal femoral epiphysis (TDL_{CP} ≥ 20.0 cm), the proximal epiphysis in the radius (TDL_{CP} ≥ 22.4 cm, 108 gestation days, 78% GP_{CP}), the epiphysis in the metacarpi and metatarsi, the distal epiphysis of the radius and humerus of fetuses (TDL_{CP} = 22.8 cm, 109 gestation days, 79% GP_{CP}), and the proximal and distal epiphysis of the tibia (TDL_{CP} ≥ 24.1 cm, 114 gestation days, 82% GP_{CP}).

The secondary centers with a more delayed mineralization onset were the proximal epiphysis of the humerus, distal epiphysis of the ulna and fibula, and epiphysis of proximal and middle phalanges of the forepaw and hind paw, being first observed in fetuses with TDL_{CP} ≥ 29.3 cm (132 gestation days, 95% GP_{CP}). Signs of mineralization in other epiphyseal ossification centers were not observed.

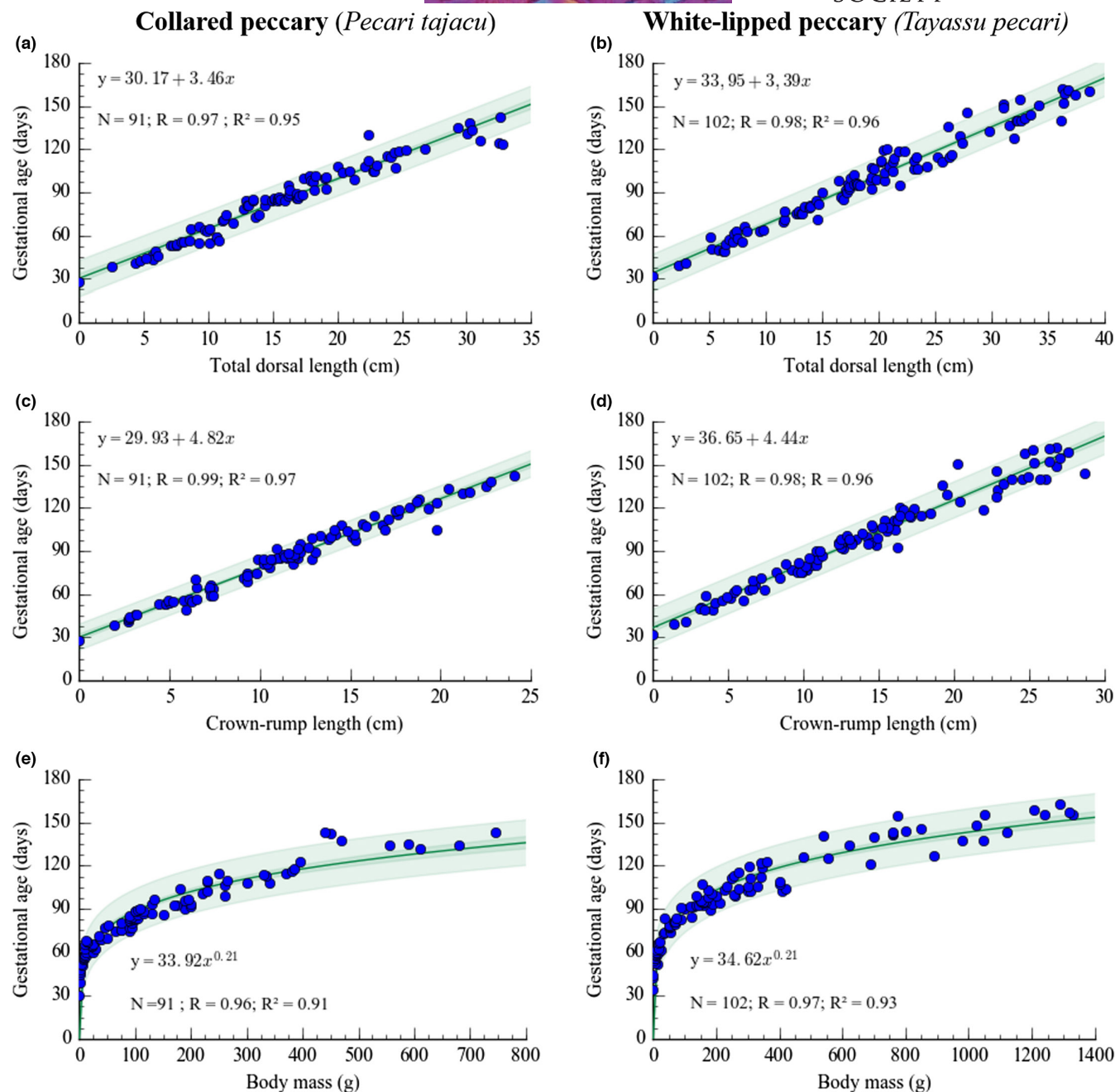


FIGURE 4 Relationship between total dorsal length (TDL), crown-rump length (CRL), and body mass with gestational age in 53 collared (*Pecari tajacu*; left column) and 61 white-lipped peccary (*Tayassu pecari*; right column) embryos/fetuses: (a, b) TDL and gestational age; (c, d) CRL and gestational age; (e, f) body mass and gestational age. Prediction intervals (light green band) and confidence intervals (green dark band).

In the WLP, the distal epiphyses of the radius, femur, and tibia were the first mineralized secondary centers observed, in fetuses with $TDL_{WLP} = 21.3$ cm (106 gestation days, 67% GP_{WLP}) (Figure 6b,d). The next secondary ossification centers to show signs of mineralization were the epiphysis of the proximal phalanx of the hind paw ($TDL_{WLP} \geq 23.1$ cm, 112 gestation days, 71% GP_{WLP}), the distal humeral epiphysis and proximal epiphysis of the femur ($TDL_{WLP} \geq 26.1$ cm, 122 gestation days, 77% GP_{WLP}), the epiphysis of metacarpi, metatarsi, and the proximal epiphysis of tibia

($TDL_{WLP} \geq 26.4$ cm, 123 gestation days, 78% GP_{WLP}). The proximal radial epiphysis, the epiphysis of the proximal phalange of forepaw, and the distal fibular epiphysis appeared in fetuses with $TDL_{WLP} \geq 27.4$ cm (127 gestation days, 80% GP_{WLP}). The last secondary centers detected were the head and great tubercle of the humerus, distal ulnar epiphysis, and epiphysis of middle phalanges of the forepaw and hind paw ($TDL_{WLP} \geq 31.0$ cm, 139 gestation days, 87% GP_{WLP}). Signs of mineralization in other epiphyseal ossification centers were not observed.

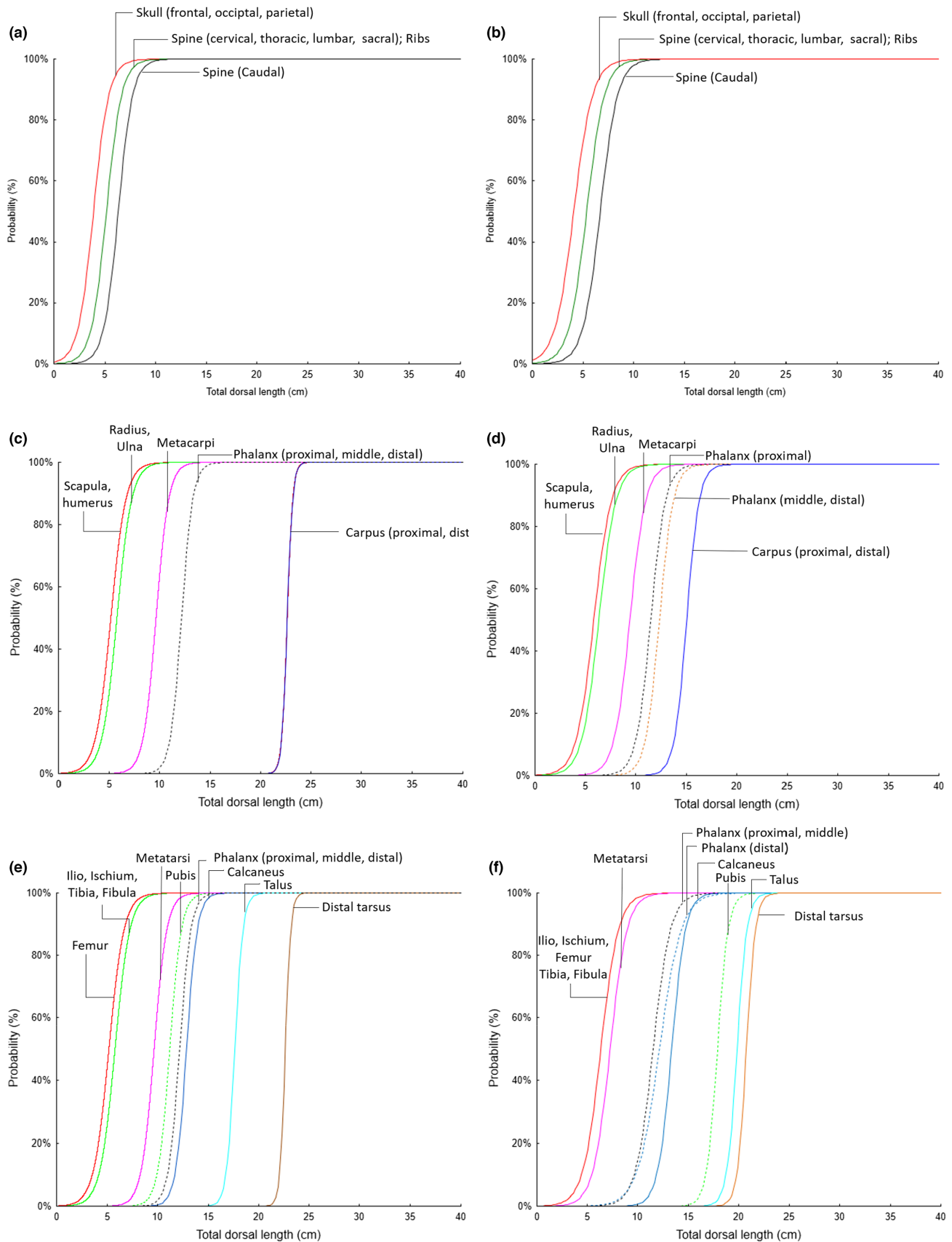
Collared peccary (*Pecari tajacu*)White-lipped peccary (*Tayassu pecari*)

FIGURE 5 Probability curves for the occurrence of skeletal bone mineralization in 53 collared (*Pecari tajacu*; left column) and 61 white-lipped peccary (*Tayassu pecari*; right column) embryos/fetuses in relation to the total dorsal length (TDL): (a, b) in the axial skeleton, and (c, d) in the thoracic and (e, f) pelvic limb.

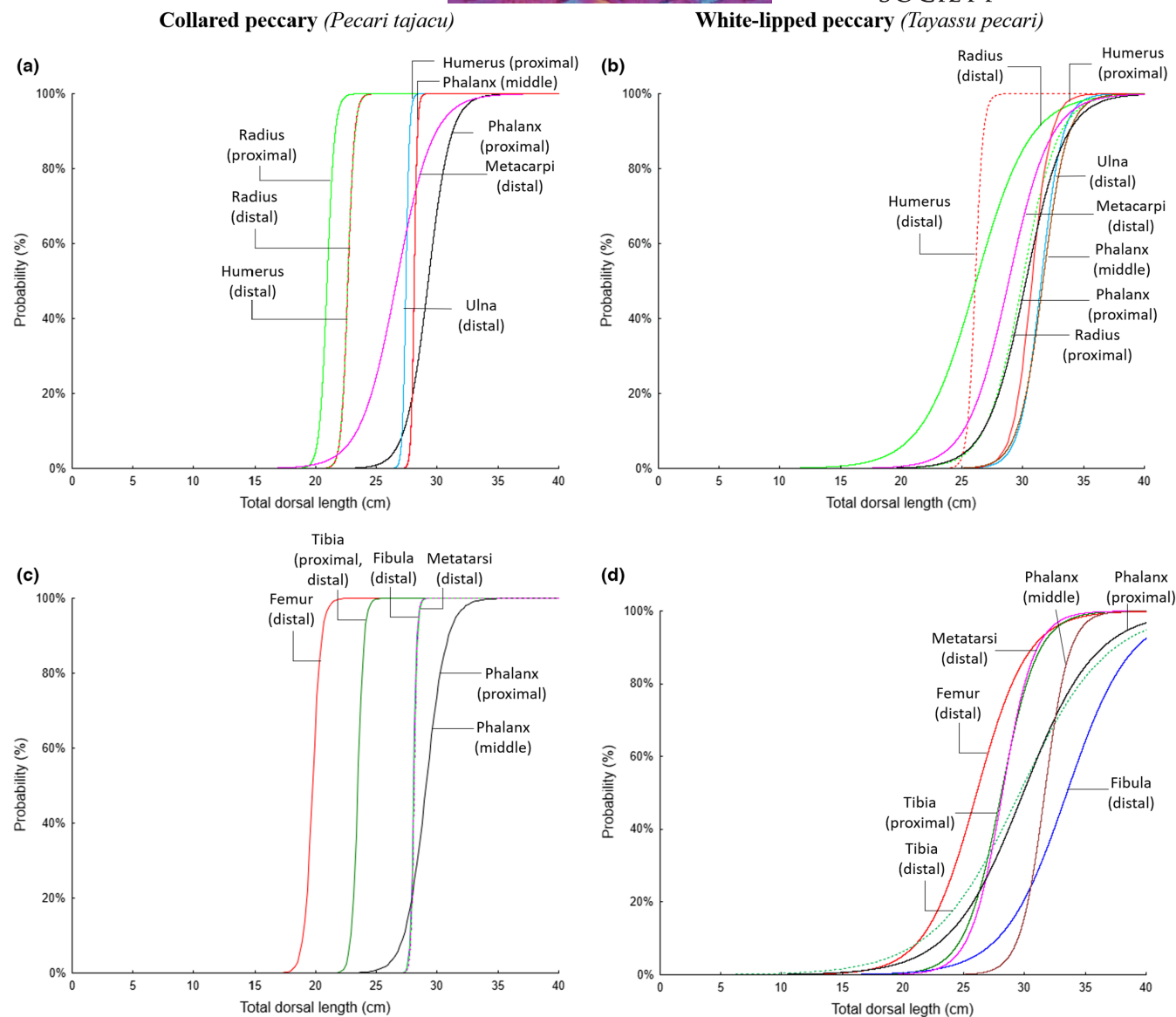


FIGURE 6 Probability curves for the occurrence of mineralization of the secondary centers of ossification in 53 collared (*Pecari tajacu*; left column) and 61 white-lipped peccary (*Tayassu pecari*; right column) embryos/fetuses in relation to the total dorsal length (TDL): (a, b) in the thoracic and (c, d) pelvic limb.

Advanced fetuses of both peccaries (>75% GP) showed well-developed secondary ossification centers in long bones. Advanced CP fetuses presented 60% (15/25) of the secondary centers observed in adult domestic pigs, while WLP presented 68% (17/25). Table S2 shows the reported secondary ossification centers of large bones in newborns and adults in the CP, WLP, domestic species, and humans.

3.4 | Allometric relationships

The diaphysis growth was not isometric; thus, the long bones have not developed in similar proportions throughout pregnancy (Figure 7). During the early pregnancy stage in the CP, the femur

and humerus were the longest bones, followed by tibia and radius. In the early WLP fetal development, the femur and tibia were the longest bones, followed by humerus and radius; however, in advanced fetuses of both species, the tibia was the longest bone, followed by the femur, the humerus, and the radius. Whereas the stylopod maintained the same length in both members (ratio femur/humerus of 1.00 ± 0.03 in the CP and 1.02 ± 0.06 in the WLP), the zeugopod in the pelvic member was more developed than in the thoracic member (ratio radius/tibia of 0.74 ± 0.03 in the CP and 0.74 ± 0.03 in the WLP) (Figure 7).

The long bones of the stylopod and the zeugopod (humerus, radius, femur, and tibia) of peccaries had a high width/length ratio at the beginning of gestation but decreased throughout the fetal development, reducing their sturdiness (Figure S1).

TABLE 2 Logistic equations [$y = \exp(\text{intercept} + \text{estimate} \times x) / (1 + \exp(\text{intercept} + \text{estimate} \times x))$] for the secondary ossification centers in forelimb and hindlimb parameters in 53 collared (*Pecari tajacu*; left column) and 61 white-lipped peccary (*Tayassu pecari*; right column) embryos/fetuses

Bones	Collared peccary (N = 53)				White-lipped peccary (N = 61)			
	Intercept	Estimate	Chi-square (df)	p value	Intercept	Estimate	Chi-square (df)	p value
Ossification Center (forelimb)								
Humerus (proximal)	-225.022	8.005	37.437 (1)	<0.001	-39.838	1.296	52.2067 (1)	<0.001
Humerus (distal)	-83.945	3.707	55.115 (1)	<0.001	-81.416	3.122	65.1003 (1)	<0.001
Radius (proximal)	-67.366	3.218	58.927 (1)	<0.001	-20.347	0.680	40.8044 (1)	<0.001
Radius (distal)	-83.945	3.707	55.115 (1)	<0.001	-11.805	0.451	46.1618 (1)	<0.001
Ulna (distal)	-190.508	6.946	37.193 (1)	<0.001	-36.302	1.152	27.3734 (1)	<0.001
Metacarp	-17.857	0.670	31.819 (1)	<0.001	-16.802	0.583	48.6199 (1)	<0.001
Proximal phalanx	-31.872	1.089	23.252 (1)	<0.001	-18.67	0.617	47.2381 (1)	<0.001
Middle phalanx	-225.022	8.005	37.436 (1)	<0.001	-31.554	0.997	45.7150 (1)	<0.001
Ossification Center (hind limb)								
Femur (distal)	-55.659	2.820	60.050 (1)	<0.001	-12.424	0.477	52.8469 (1)	<0.001
Tibia (proximal)	-92.587	3.947	53.715 (1)	<0.001	-18.754	0.668	54.4561 (1)	<0.001
Tibia (distal)	-92.587	3.947	53.715 (1)	<0.001	-8.258	0.279	30.9475 (1)	<0.001
Fibula (distal)	-220.720	7.864	36.945 (1)	<0.001	-12.872	0.385	24.0075 (1)	<0.001
Metatarsi	-220.380	7.841	37.435 (1)	<0.001	-21.378	0.759	52.5774 (1)	<0.001
Proximal phalanx	-34.543	1.188	27.730 (1)	<0.001	-10.041	0.336	33.4424 (1)	<0.001
Middle phalanx	-34.543	1.188	27.730 (1)	<0.001	-31.554	0.997	45.7150 (1)	<0.001

3.5 | Bone measurements and gestational age

In the CP and WLP, all biometric measurements showed a strong positive association with TDL ($r^2 > 0.79$ and $r^2 > 0.80$, respectively; $p < 0.01$). The skull measurements showed a strong association with TDL_{CP} ($r^2 > 0.95$, $p < 0.01$), with OFD and HC presenting the highest coefficient of determination ($r^2 = 0.96$, $p < 0.01$) (Figure S2c,e). The strongest associations with TDL_{CP} was observed in total length of the scapula ($r^2 = 0.98$, $p < 0.01$; Figure S3a), the total length of the humerus in the stylopod and zeugopod of the forepaw ($r^2 = 0.98$, $p < 0.01$) (Figure S4a), and the mineralized diaphysis of the metacarpus ($r^2 = 0.96$, $p < 0.01$) (Figure S7a) in the autopod of the forepaw.

In the hind paw of CP, the strongest association with TDL_{CP} was observed in total length and mineralized part of the ilium, width of the ischium, and length of the pubis ($r^2 = 0.97$, $p < 0.01$) (Figure S9a,b, S10c,d), the total length and diaphysis of the femur in the stylopod and zeugopod ($r^2 = 0.98$, $p < 0.01$) (Figure S11a,b), and the mineralized diaphysis of the metatarsi in the autopod ($r^2 = 0.96$, $p < 0.01$) (Figure S14a).

In WLP, the skull measurements also showed a strong positive association with TDL_{WLP} ($r^2 > 0.90$, $p < 0.01$); however, the BPD was the measurement with the highest coefficient of determination ($r^2 = 0.97$, $p < 0.01$). The strongest associations with TDL_{WLP} were observed in total length and the mineralized part of the scapula ($r^2 = 0.97$, $p < 0.01$; Figure S3d,e), the total length of the humerus

in the stylopod and zeugopod of the forepaw ($r^2 = 0.97$, $p < 0.01$) (Figure S4f), and the mineralized diaphysis of the metacarpus ($r^2 = 0.96$, $p < 0.01$) (Figure S7c) in the autopod of the forepaw.

In the hind paw of WLP, the strongest association with TDL_{WLP} were observed in total length of the ilium ($r^2 = 0.96$, $p < 0.01$) (Figure S9d), the femoral diaphysis ($r^2 = 0.97$, $p < 0.01$) (Figure S11g), and the mineralized diaphysis of the metatarsi in the autopod ($r^2 = 0.94$, $p < 0.01$) (Figure S14c). All graphs for these associations are presented in Figures S2–S15.

4 | DISCUSSION

The timing of the main events during the embryonic and fetal skeletal development in two closely phylogenetically related species, CP, and WLP, is similar. In both species, advanced fetuses showed mineralization in all primary ossification centers and most secondary centers of long bones. Their early development of the skeletal system agrees with the observed early development of external morphology and thoracic and abdominal organs in these species (Andrade, Monteiro, El Bizri, et al., 2018; Mayor et al., 2019). Precocial species are characterized by a high fetal growth rate, delivering at term well-developed neonates with low parental dependence. Thus, peccary neonates show both a high ability for sensorial processing to receive stimuli from the environment (Andrade, Monteiro, El Bizri, et al., 2018; Mayor et al., 2019) and a well-developed musculoskeletal

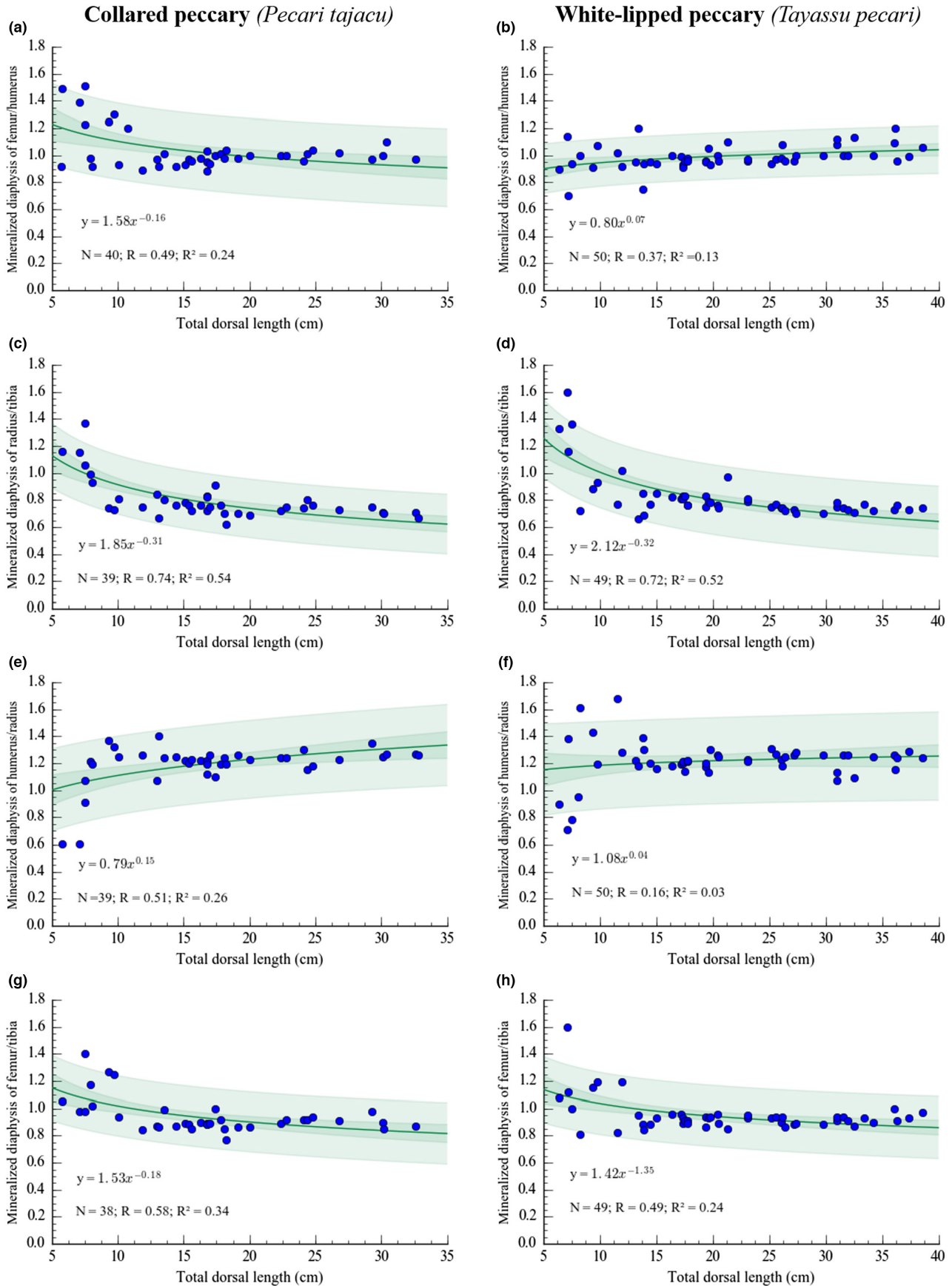


FIGURE 7 Allometric relationships between diaphyseal lengths of long bones in 53 collared (*Pecari tajacu*; left column) and 61 white-lipped peccary (*Tayassu pecari*; right column) embryos/fetuses, related to the total dorsal length (TDL): (a, b) femur versus humerus, (c, d) radius versus tibia, (e, f) humerus versus radius, and (g, h) femur versus tibia. Prediction intervals (light green band) and confidence intervals (green dark band).

system that provides a higher ability for locomotion, which is of paramount importance for foraging and scape predation (Anthwal & Thompson, 2016; Sarko et al., 2011).

Ultrasonography is widely used in many domestic species to measure fetal development using CRL as a surrogate of gestational age (Daneze et al., 2012; Ogata et al., 1999). In both peccary species, CRL and TDL showed a strong correlation with gestational age. The CRL is considered one of the selection parameters to calculate the gestational period, especially in the first stages of pregnancy (Butt et al., 2014). Similarly, the TDL may be used as an index for wild species because its values are not influenced by the handling in ultrasonography (El Bizri et al., 2017; Silva et al., 2020). Thus, measuring TDL may be an alternative method to estimate the fetal length and gestational age of conceptuses, avoiding bias due to changes in a fetal position (Andrade, Monteiro, El Bizri, Vicente, et al., 2018).

First signs of bone mineralization were observed after 30% GP_{CP} (42 gestation days) and 32% GP_{WLP} (52 gestation days). The first US signs of skeletal mineralization in both peccaries begin after the differentiation of limbs and genitalia, and formation of eyelid buds, and before the formation of the outer ear, fusion of eyelids, and presence of hooves (Andrade, Monteiro, El Bizri, et al., 2018; Mayor et al., 2019). In both species, the first mineralized structure was the skull, allowing cranial biometry to function as early markers of the gestational age. The high correlation of biparietal diameter with gestational age reinforces this parameter as a reliable and feasible indicator of the fetal age, as previously observed in these species (Mayor et al., 2005), and other domestic ungulates, such as domestic pig (*Sus domesticus*; Daneze et al., 2012), sheep (*Ovis aries*; Metodiev et al., 2012), and cattle (*Bos taurus*; Menezes et al., 2011). The skull is one of the first structures to become mineralized to protect the soft tissues of the brain during its early development (Richtsmeier & Flaherty, 2013).

In peccaries, the first US signs of mineralization of the skull occur at the end of the initial third of the gestational period, similar to those observed in domestic pigs at 37 days of gestation (26% of the GP; Daneze et al., 2012) and sheep (29% GP; Harris, 1937), other precocial wild species, such as lowland paca (*Cuniculus paca*; 28% GP; Silva et al., 2020), and even altricial species, such as the owl monkey (*Aotus azarai infulatus*; 26% GP; Monteiro et al., 2011), humans (26% GP; Rosignoli et al., 2010; Jin et al., 2016), and marmosets (*Callithrix jacchus*; 27% GP; Phillips, 1976). Thus, the timing of first signs of bone mineralization is similar in precocial and altricial species, showing that the early embryo and fetal development of the skeletal system are similar in mammals (Evans & Sack, 1973).

The development of the thoracic and pelvic limbs was evidenced by the early appearance of mineralization in all long bones in both peccaries (36% GP_{CP} and 35% GP_{WLP}), like that described in the lowland paca (33% GP; Silva et al., 2020) and slightly late in comparison with the sheep (30%; Harris, 1937). In altricial animals, such as rabbits (*Oryctolagus cuniculus*) and laboratory rats (*Ratus norvegicus*), the long bones were observed only in more advanced fetuses with 60% (Kamal, 2019) and 75% GP (Patton & Kaufman, 1995), respectively.

Muscular maturation requires the formation of resistant bones for the muscle insertion and resistance to traction forces (Muir, 2000;

Sinowatz, 2010). During the intrauterine period, the myotomes of the somites promote the formation of epaxial and hypaxial muscles, which are related to the development of bone structures in the axial skeleton that help in the positioning and insertion of the developing muscles (Gilbert, 2000; Sinowatz, 2010). Regarding the appendicular skeleton, the bone development of limbs offers support to the musculature, which provides the impulse during locomotion, particularly important in early life stages when predation risk is higher and when newborns should have a strong flee reaction to predators (Getty, 1986; Searfoss, 1995).

Signs of mineralization in the metacarpi/metatarsi and phalanges in both peccaries (metacarpi/metatarsi 46% GP_{CP} and 37% GP_{WLP}; phalanges 55% GP_{CP} and 46% GP_{WLP}) were again slightly delayed compared to the sheep (metacarpi/metatarsi 32% GP; phalanges 42% GP; Harris, 1937). In altricial animals, mineralization of the autopod was observed at 73% GP in rabbits (Kamal, 2019) and 81% GP in the laboratory rat (Patton & Kaufman, 1995). The early development of the autopod is essential in unguligrade and cursorial animals. These species have elongated limbs and phalanges and support the bodyweight on the fingers. The early development of the autopod with a carrying capacity allows running away from predators and traveling long distances with minimal energy expenditure, offering independence in locomotion at an early age (Hildebrand, 1980, 2006; Varela, 2010).

Secondary ossification centers showed substantial variation in diameter in fetuses in similar gestational periods. Thus, the gestational period was best estimated by the appearance or absence of epiphyseal ossification centers, as observed in humans in distal epiphyses of the humerus and femur (Donne et al., 2005). In both peccaries, the earliest mineralization in secondary centers of long bones begins in the final third of the gestational period, including the distal epiphysis of the femur (72% GP_{CP}), and the distal epiphyses in radius, femur, and tibia (67% GP_{WLP}). At this gestational stage, fetuses have already important many external characteristics well-developed, such as skin, tactile pelage, opened eyelids, and tooth eruption (Andrade, Monteiro, El Bizri, et al., 2018; Mayor et al., 2019).

In vertebrates, the development of the phenotype muscle is highly associated with the development of bone eminences. Although bones present independent development from the muscles, secondary ossification centers depend on the growth of the musculature (Huang, 2017). The late appearance of secondary centers for the formation of eminences occurs after muscle growth and the appearance of the insertion tendon. The generation of mechanical forces strengthen the tissue functionality, regulating the musculoskeletal development and promoting the development of the ossification centers (Felsenthal & Zelzer, 2017). Precocial species are characterized by having well-developed primary and secondary ossification centers after birth; while altricial species usually present poor development of secondary ossification centers (Li & Smith, 2019; Modina et al., 2017).

In our study, most advanced CP and WLP fetuses presented 60% (15/25) and 68% (17/25) of the secondary centers, respectively. Due to the scarce information on the secondary centers in peccaries,

this percentage was calculated based on observations in the adult domestic pigs (Barone, 2010; Dyce et al., 2010). Peccary piglets presented a higher percentage of secondary ossification centers compared with domestic piglets (52%, 13/25), and fewer numbers than newborns of cattle (92%, 23/25) and horses (80%, 20/25). In contrast, altricial species, such as carnivores (dogs and cats) and humans, present 0% (0/31) and only 7.4% (2/27) secondary ossification centers at birth, respectively (Barone, 2010; Dyce et al., 2010). Thus, the development of secondary ossification centers is associated with lower motor skills at birth (Young & Shapiro, 2018). In addition, variations in the number and appearance of ossification centers exhibit a gradual spectrum of levels of development among species modulated by the various adaptive strategies to optimize the survival rate of newborns adopted by different species (Derrickson, 1992).

We did not observe mineralization of the patella in advanced fetuses of either CP or WLP. Most placental mammals have a mineralized patella a few weeks after the birth, such as the pig (Wenham et al., 1973) and the rabbit (Bland & Ashhurst, 1997), or even after months, such as human and great apes (Smith et al., 2020). However, few mammals' species show a mineralized patella at the end of gestation, such as the lowland paca (Silva et al., 2020) and the goat (Parmar et al., 2009). This sesamoid bone promotes extension of the knee joint and stability during walking, supporting the locomotion (Getty, 1986). As observed in pigs, the ossification center of the patella in peccaries likely occurs a few weeks after birth.

The early bone development is similar in altricial and precocial animals, with the development of the axial skeleton and primary ossification centers of long bones that allow first muscle insertions (Muir, 2000; Sinowatz, 2010). However, divergences in bone development are observed as gestation progresses, and precocial species show a more complete bone gestational development in primary and secondary ossification centers than altricial species (Li & Smith, 2019; Modina et al., 2019; Phillips, 1976; Silva et al., 2020).

In the Amazon region, the main natural predators of peccaries are large felids (*Puma concolor* and *Panthera onca*) (Cavalcanti & Gese, 2010; Keuroghlian et al., 2013), who prefer to predate on vulnerable individuals, such as newborns (Crawshaw & Quigley, 1991; Mayer & Wetzell, 1987). Our results suggest that likely in response to high predation risks at an early age, peccary newborns develop early autonomous locomotion to maximize their ability to escape predation (Mayor et al., 2019). In addition, to increase the survival rate of peccary neonates, adults present anti-predation behaviors and protect piglets in cooperative care of newborns conducted by the whole herd (Rampim et al., 2020; Tiepolo & Tomas, 2006). The early skeleton development is also important for newborns to follow the herd's foraging activity, which covers large areas due to the species' nomadic behavior (Garcia et al., 2009; Sowls, 1997).

The altricial/precocial dichotomous classification does not cover the particularities observed in the fetal development of mammal diversity. Thus, the perspective of a gradual spectrum of fetal development is more reliable and considers variations and nuances of precociality and altriciality according to the species' morphological characteristics and life history (Derrickson, 1992). The description

of the main chronological events during the development of the skeletal system in the collared and the WLP is useful for gestational management and improves our understanding of the life history strategies of precocial and altricial mammals in the wild.

AUTHOR CONTRIBUTIONS

P.M. and F.O.B.M conceived the study. P.M., R.E.B, J.V., P.P.P., and H.R.E.B. conducted the fieldwork. T.H.S.P., G.P.S., and S.E.R.M. participated in data collection and analysis. T.H.S.P., P.M., and F.O.B.M. wrote the manuscript. H.R.E.B., L.N.C., C.L.P. revised the manuscript.

ACKNOWLEDGMENTS

We sincerely thank all the people from the community of Nueva Esperanza in the Yavarí-Mirín River, and from the communities of Nova Jerusalém, Boa Esperança, Bom Jesus do Baré, São José do Urini, and Belo Monte in the Amanã Sustainable Development Reserve, who actively participated in data collection. Communal participation is an important step in the development of wildlife management. We are especially thankful for the institutional support provided by the Gordon and Betty Moore Foundation (number 5344), Instituto de Investigaciones de Trópico y de Altura, the Museo de la Universidad Nacional de la Amazonía Peruana, and the Dirección General de Flora y Fauna Silvestre from Peru. This work was supported by the National Council of Technological and Scientific Development (CNPq, award numbers 441435/2007-3, 452908/2016-7, 201475/2017-0, and Edital n° 016/2014 PPP-CNPq), Fundação de Amparo à Pesquisa do Estado do Amazonas (FAPEAM, Edital n° 016/2014 PPP-CNPq), Coordenação de Aperfeiçoamento de Pessoal de Nível Superior (CAPES, protocol N° 23038.005350/2018-78) and the Earthwatch Institute. The authors have no conflict of interest to declare.

DATA AVAILABILITY STATEMENT

Authors agree to make data and materials supporting the results or analyses presented in their paper available upon reasonable request.

ORCID

Frederico Ozanan Barros Monteiro  <https://orcid.org/0000-0002-1406-9979>

REFERENCES

- Andrade, R.D.S., Monteiro, F.O.B., El Bizri, H.R., Vicente, W.R.R., Guimarães, D.A.A. & Mayor, P. (2018) Fetal development of the Poeppig's woolly monkey (*Lagothrix poeppigii*). *Theriogenology*, 8, 34–43.
- Andrade, R.S., Monteiro, F.O.B., El Bizri, H.R., Pantoja, L., Bodmer, R., Valsecchi, J. et al. (2018) Embryonic and fetal development of the white-lipped peccary (*Tayassu pecari*). *Theriogenology*, 119, 163–174.
- Anthwal, N. & Thompson, H. (2016) The development of the mammalian outer and middle ear. *Journal of Anatomy*, 228(2), 217–232.
- Barone, R. (2010) *Anatomie comparée des mammifères domestiques, Tome I, Osteologie*, 5th edition. Paris: Ed Vigot Frères.
- Bland, Y.S. & Ashhurst, D.E. (1997) Fetal and postnatal development of the patella, patellar tendon and suprapatella in the rabbit: changes

- in the distribution of the fibrillar collagens. *Journal of Anatomy*, 190, 327–342.
- Butt, K., Lim, K. & DIAGNOSTIC IMAGING COMMITTEE. (2014) Determination of gestational age by ultrasound. *Journal of Obstetrics and Gynaecology Canada*, 36(2), 171–181.
- Cavalcanti, S.M.C. & Gese, E.M. (2010) Kill rates and predation patterns of jaguars (*Panthera onca*) in the southern Pantanal. *Brazilian Journal of Mammalogy*, 91, 722–736.
- Clancy, B., Darlington, R.B. & Finlay, B.L. (2001) Translating developmental time across mammalian species. *Neuroscience*, 105, 7–17.
- Crawshaw, P.G., Jr. & Quigley, H. (1991) Jaguar spacing, activity and habitat use in a seasonally flooded environment in Brazil. *Journal of Zoology*, 223, 357–370.
- Daneze, E.R., Léga, E. & Pinto, M.L. (2012) Fetometria ultrassonográfica em porcas gestantes como método complementar para avaliação da morfologia e determinação da idade fetal. *Nucleus Animalium*, 4, 19–29.
- Derrickson, E.M. (1992) Comparative reproductive strategies of altricial and precocial eutherian mammals. *Functional Ecology*, 6, 57–65.
- Donne, H.D., Jr., Faúndes, A., Tristão, E.G., de Sousa, M.H. & Urbanetz, A.A. (2005) Sonographic identification and measurement of the epiphyseal ossification centers as markers of fetal gestational age. *Journal of Clinical Ultrasound*, 33, 394–400.
- Dyce, K.M., Sack, W.O. & Wensing, C.J.G. (2010) *Textbook of veterinary anatomy*, 4th edition. St Louis: Saunders Elsevier.
- El Bizri, H.R., Monteiro, F.O.B., Andrade, R.S., Valsecchi, J., Guimarães, D.A.A. & Mayor, P. (2017) Embryonic and fetal morphology in the lowland paca (*Cuniculus paca*): a precocial hystricomorph rodent. *Theriogenology*, 104, 7–17.
- Evans, H.E. & Sack, W.O. (1973) Prenatal development of domestic and laboratory mammals: growth curves, external features and selected references. *Anatomia, Histologia, Embryologia: Journal of Veterinary Medicine Series C*, 2, 11–45.
- Fang, T., Bodmer, R., Puertas, P. et al. (2008) *Certificación de pieles de pecarías (Tayassu tajacu y T. pecari) en la Amazonía peruana: Una estrategia de conservación y manejo de fauna silvestre en la Amazonía peruana*. Lima, Peru: Wust Editions-Darwin Institute.
- Felsenthal, N. & Zelzer, E. (2017) Mechanical regulation of musculoskeletal system development. *Development*, 144, 4271–4283.
- Francioli, A.L.R., Ambrósio, C.E., Oliveira, M.F., Morini, A.C., Favaron, P.O., Machado, M.R.F. et al. (2011) Os histricomorfos sul-americanos: uma análise comparativa do desenvolvimento embrionário. *Pesquisa Veterinária Brasileira*, 31, 441–446.
- Garcia, A.R., Kahwage, P.R. & Ohashi, O.M. (2009) Aspectos reprodutivos de caititus (*Tayassu tajacu*). *Revista Brasileira de Reprodução Animal*, 33, 71–81.
- Getty, R. (1986) *SISSON; GROSSMAN. Anatomia dos Animais Domésticos*. 5th edition. Rio de Janeiro: Guanabara Koogan.
- Gilbert, S.F. (2000) *Developmental biology*, 6th edition. Sunderland, MA: Sinauer Associates.
- Gongora, J., Reyna-Hurtado, R., Beck, H., Taber, A., Altrichter, M. & Keuroghlian, A. (2011) *Pecari tajacu*. The IUCN red list of threatened species 2011, e.T41777A10562361. <https://doi.org/10.2305/IUCN.UK.2011-2.RLTS.T41777A10562361.en>
- Gottdenker, N.L. & Bodmer, R.E. (1998) Reproduction and productivity of white-lipped and collared peccaries in the Peruvian Amazon. *Journal of Zoology*, 245, 423–430.
- Harris, H.A. (1937) The foetal growth of the sheep. *Journal of Anatomy*, 71, 516–527.
- Hildebrand, M. (1980) The adaptive significance of tetrapod gait selection. *American Zoology*, 20, 255–267.
- Hildebrand, M. (2006) *Análise da estrutura dos vertebrados (tradução)*. São Paulo: Atheneu.
- Huang, A.H. (2017) Coordinated development of the limb musculoskeletal system: tendon and muscle patterning and integration with the skeleton. *Developmental Biology*, 429, 420–428.
- International Committee on Veterinary Embryological Nomenclature. (2017) *Nomina Embryologica Veterinaria*. Zurich Ithaca, New York: World Association of Veterinary Anatomists (WAVA).
- Jin, S.W., Sim, K.B. & Kim, S.D. (2016) Development and growth of the normal cranial vault: an embryologic review. *Journal of Korean Neurosurgery Society*, 59, 192–196.
- Kamal, B.M. (2019) Sequential pattern of prenatal ossification in the fore limb bones in white New Zealand rabbits by double stained techniques and computed tomography. *PSM Veterinary Research*, 4, 24–35.
- Karami, M., Moradi, M., Khazaei, M., Modaresi, M.R., Asadi, K. & Soleimani, M. (2016) Detection of secondary ossification centers by sonography. *Advanced Biomedical Research*, 5, 1–3.
- Keuroghlian, A., Desbiez, A., Reyna-Hurtado, R., Altrichter, M., Beck, H., Taber, A. et al. (2013) *Tayassu pecari*. The IUCN red list of threatened species, e.T41778A44051115.
- Li, P. & Smith, K.K. (2019) Comparative skeletal anatomy of neonatal ursids and the extreme altriciality of the giant panda. *Journal of Anatomy*, 236, 724–736.
- Mahoney, B.S., Callen, P.W. & Filly, R.A. (1985) The distal femoral epiphyseal ossification center in the assessment of third-trimester menstrual age: sonographic identification and measurement. *Radiology*, 155, 201–204.
- Mayer, J.J. and Wetzel, R.M. (1987) *Tayassu pecari*. Mammalian species, 293, 1–7.
- Mayor, P., Lopez-Gatius, F. & López-Béjar, M. (2005) Ultrasonography within the reproductive management of collared peccary (*Tayassu tajacu*). *Theriogenology*, 63, 1832–1843.
- Mayor, P., Fenech, M., Bodmer, R.E. & López-Béjar, M. (2006) Ovarian features of the wild collared peccary (*Tayassu tajacu*) from Peruvian north-eastern Amazon. *General and Comparative Endocrinology*, 147, 268–275.
- Mayor, P., Guimaraes, D.A., Lopez-Gatius, F. & López-Béjar, M. (2006) First postpartum estrus and pregnancy in the female collared peccary (*Tayassu tajacu*) from the Amazon. *Theriogenology*, 66, 2001–2007.
- Mayor, P., Bodmer, R. & López-Béjar, M. (2009) Reproductive performance of the wild white-lipped peccary (*Tayassu pecari*) in the Peruvian Amazon. *European Journal of Wildlife Research*, 55, 631–634.
- Mayor, P., El Bizri, H., Bodmer, R. & Bowler, M. (2017) Assessment of mammal reproduction for hunting sustainability through community-based sampling of species in the wild. *Conservation Biology*, 31, 912–923.
- Mayor, P., Silva, G.P., Andrade, R.S., Monteiro, F.O.B. & El Bizri, H.R. (2019) Embryonic and fetal development of the collared peccary (*Pecari tajacu*). *Animal Reproduction Science*, 208, 106–123.
- Menezes, M.C., Léga, E. & Coelho, L.A.F. (2011) Utilização da ultrassonografia por via transretal em vacas da raça girolando para acompanhamento do desenvolvimento embrionário e/ou fetal 26 a 181 dias de gestação. *Nucleus Animalium*, 3, 37–60.
- Metodiev, N., Dimov, D., Ralchev, I. & Raicheva, E. (2012) Measurement of foetal growth via transabdominal ultrasonography during first half of pregnancy at ewes from synthetic population Bulgarian milk. *Bulgarian Journal of Agricultural Science*, 18, 493–500.
- Modina, S.C., Veronesi, M.C., Moiola, M., Meloni, T., Lodi, G., Bronzo, V. et al. (2017) Small-sized newborn dogs skeletal development: radiologic, morphometric, and histological findings obtained from spontaneously dead animals. *BMC Veterinary Research*, 13(175), 1–10.
- Modina, S.C., Andreis, M.E., Moiola, M. & Di Giancamillo, M. (2019) Age assessment in puppies: coming to terms with forensic requests. *Forensic Science International*, 297, 8–15.
- Monteiro, F.O.B., Coutinho, L.N., Silva, G.A., Castro, P.H.G., Maia, C.E., Silva, K.S.M. et al. (2011) Ultrasound evaluation of pregnancy in owl monkey (*Aotus azarai infulatus*). *Animal Reproduction*, 8, 40–46.
- Moradi, B., Ghanbari, A., Rahmani, M., Kazemi, M.A., Tahmasebpour, A.R. & Shakiba, M. (2019) Evaluation of bi-iliac distance and timing of ossification of sacrum by sonography in the second trimester of pregnancy. *Iranian Journal of Radiology*, 16, e79940.

- Muir, G.D. (2000) Early ontogeny of locomotor behavior: a comparison between altricial and precocial animals. *Brain Research Bulletin*, 53, 719–726.
- Ogata, Y., Nakao, T., Takahashi, K., Abe, H., Misawa, T., Urushiyama, Y. et al. (1999) Intrauterine growth retardation as a cause of perinatal mortality in Japanese black beef calves. *Journal of Veterinary Medicine*, 46, 327–334.
- Parmar, V.K., Patel, K.B., Desai, M.C., Mistry, J.N. & Chaudhary, S.S. (2009) Radiographic study on the first appearance of ossification centers of bones in the goat fetuses: the pelvic limb. *Indian Journal of Field Veterinarians*, 4, 6–10.
- Patton, J.T. & Kaufman, M.H. (1995) The timing of mineralization of the limb bones, and growth rates of various long bones of the fore and hind limbs of the prenatal and early postnatal laboratory mouse. *Journal of Anatomy*, 186, 175–185.
- Phillips, I.R. (1976) Skeletal development in the foetal and neonatal marmoset (*Callithrix jacchus*). *Laboratory Animals*, 10, 317–333.
- Rampim, L.E., Sartorello, L.R., Fragoso, C.E., Habersfeld, M. & Devlin, A.L. (2020) Antagonistic interactions between predator and prey: mobbing of jaguars (*Panthera onca*) by white-lipped peccaries (*Tayassu pecari*). *Acta Ethologica*, 23, 45–48.
- Richtsmeier, J.T. & Flaherty, K. (2013) Hand in glove: brain and skull in development and dysmorphogenesis. *Acta Neuropathologica*, 125, 469–489.
- Roots, C.G. (1966) Notes on the breeding of the white-lipped peccaries at Dudley zoo. *International Zoo Yearbook*, 6, 198–199.
- Rosignoli, L., Tonni, G. & Centini, G. (2010) Cranial development in the first trimester: the use of 3D in the study of complex structures. *Imaging in Medicine*, 2, 251–257.
- Sarko, D.K., Rice, F.L. & Reep, R.L. (2011) Mammalian tactile hair: divergence from a limited distribution. *Annals of the New York Academy of Sciences*, 1225, 90e100.
- Searfoss, G. (1995) *Skulls and bones: a guide to the skeletal structures and behavior of north American mammals*, 6th edition. Mechanicsburg, PA: Stackpole Books.
- Silva, G.P., Monteiro, F.O.B., Pereira, T.H.S. et al. (2020) Fetal bone development in the lowland paca (*Cuniculus paca*, Rodentia, Cuniculidae) determined using ultrasonography. *Journal of Anatomy*, 237, 105–118.
- Sinowatz, F. (2010) Musculo-skeletal system. In: Hyttel, P., Sinowatz, F. & Vejsted, M. (Eds.) *Domestic animal embryology*. Edinburgh, UK: Saunders Elsevier.
- Smith, T., DeLeon, V., Vinyard, C. & Young, J. (2020) The pectoral girdle and forelimb skeleton. In: *Skeletal anatomy of the newborn primate*, 1st edition. Cambridge: Cambridge University Press, pp. 163–190.
- Sowls, L.K. (1997) *Javelines and other peccaries: their biology, management and use*, 2nd edition. Tucson, Texas: A & M University Press.
- Tiepolo, L.M. & Tomas, W.M. (2006) *Ordem Artiodactyla*. In: Reis, N.R., Peracchi, A.L., Pedro, W.A. & Lima, I.P. (Eds.) *Mamíferos do Brasil*, 2nd edition. Edue: Londrina, pp. 293–313.
- Varela, G. (2010) Osteología y miología de Los miembros anterior e posterior del venado de campo (*Ozotoceros bezoaricus*). Tesis de grado (Licenciatura en Ciencias Biológicas), Universidad de La Republica, Uruguay. Facultad de Ciencias.
- Wenham, G., Fowler, V.R. & McDonald, I. (1973) A radiographic study of skeletal growth and development in the pig. Temporal pattern of growth. *The Journal of Agricultural Science*, 80, 125–133.
- Young, J.W. & Shapiro, L.J. (2018) Developments in development: what have we learned from primate locomotor ontogeny? *American Journal of Physical Anthropology*, 165, 37–71.

SUPPORTING INFORMATION

Additional supporting information can be found online in the Supporting Information section at the end of this article.

How to cite this article: Pereira, T.H.d., Monteiro, F.O.B., Pereira da Silva, G., Rodrigues de Matos, S.E., El Bizri, H.R. & Valsecchi, J. et al. (2022) Ultrasound evaluation of fetal bone development in the collared (*Pecari tajacu*) and white-lipped peccary (*Tayassu pecari*). *Journal of Anatomy*, 241, 741–755. Available from: <https://doi.org/10.1111/joa.13724>